

Vibrational Spectra of Phenylphosphonic and Phenylthiophosphonic Acid and their Complete Assignment

Wolfgang Förner and Hassan M. Badawi

Department of Chemistry, King Fahd University of Petroleum & Minerals (KFUPM), Dhahran 31261, Saudi Arabia

Reprint requests to W. Förner. E-mail: forner@kfupm.edu.sa

Z. Naturforsch. **2010**, 65b, 357–366; received November 1, 2009

Dedicated to Professor Rolf. W. Saalfrank on the occasion of his 70th birthday

The structures and conformational stabilities of phenylphosphonic acid and phenylthiophosphonic acid were investigated using calculations mostly at DFT/6-311G** and *ab initio* MP2/6-311G** level. From the calculations the molecules were predicted to exist in a conformational equilibrium consisting of two conformers which as enantiomers have the same energy, but rather unexpected dihedral angles XPCC (X being O or S) which are not equal to zero. The antisymmetric potential function for the internal rotation was determined for each one of the molecules. In these functions the conformers with zero dihedral angles appear to be stable minima (also optimization converges to this), but the vibrational frequency for the torsion turned out to be imaginary, indicating that they are maxima with respect to this symmetry coordinate. Only optimization without any restrictions and starting from a non-zero torsional angle converged to a real minimum with such a geometry (“non-planar”). For that minimum structure infrared and Raman spectra were calculated, and those for phenylphosphonic acid were compared to experimental data, showing satisfactory agreement. This gives confidence to present the spectra of phenylthiophosphonic acid as a prediction. The rather low intensity of the OH bands in the experimental infrared spectrum (as compared to normal organic acids) indicates rather weak hydrogen bonding. Normal coordinate calculations were carried out, and potential energy distributions were calculated for the molecules in the non (near)-planar conformations providing a complete assignment of the vibrational modes to atomic motions in the molecules. From the rather low rotational barriers we conclude, in agreement with results from the literature (for other P=O compounds) based on localized orbitals that conjugation effects are absent – or at least negligible – as compared to electrostatic and steric ones in determining the structures of the stable conformers in the phenyl derivatives. The P=O (and also the P=S) bond is highly polarized according to our analysis of Mulliken populations. The polarization turned out to be smaller in the thiophosphonic acid due to the smaller electronegativity of sulfur as compared to oxygen.

Key words: DFT and MP2 Calculations, Vibrational Spectra and Assignments, Torsional Potentials, Phenylphosphonic Acid, Phenylthiophosphonic Acid

Introduction

In the past few years, the conformational structures of many conjugated vinyl compounds with the general formula $R_2C=CRCXO$, where X could be fluorine or chlorine and R could be hydrogen or a methyl group, have been reported [1–12]. The planar *cis* and *trans* conformers in these molecules are in general stabilized by conjugation effects as compared to the non (near)-planar *gauche* conformers, which leads to a much higher rotational barrier than in the corresponding saturated molecules. In propenoyl halides, the halogen and the oxygen atoms in the carbonyl groups are

competing in determining the conformational equilibrium which leads to small energy differences between the stable conformers of such molecules. In case of 2-fluoropropenoyl fluoride [7, 11] and 2-chloropropenoyl fluoride [8], the *trans* conformer with the two halogen atoms directed away from each other was found to be more stable than the *cis* one. Furthermore, the presence of the methyl group was shown to significantly influence the conformational equilibrium mixture in the methyl-substituted propenoyl halides. For 2-methyl-2-butenoyl fluoride and chloride the *trans* form was found to be lower in energy than the *cis* form, while for 3-methyl-2-butenoyl fluoride and chloride the *cis* con-

formers were found to be more stable than the *trans* conformers [12, 13].

Some years ago we performed a study of the conformational stability of vinyl sulfonyl chloride, $\text{H}_2\text{C}=\text{CHSO}_2\text{Cl}$, and fluoride [14] because of their chemical importance and structural interest [15]. The molecules were predicted to exist predominantly in the non (near)-planar *gauche* conformations with the vinyl $\text{C}=\text{C}$ group nearly eclipsed to one of the sulfonyl $\text{S}=\text{O}$ groups again as a result of significant conjugation between the $\text{C}=\text{C}$ double bond and one of the $\text{S}=\text{O}$ double bonds [14].

To extend our study of conjugated vinyl molecules to the case of an aromatic phenyl substituent at the phosphorus atom, we investigate in the present work the conformational behavior and structural stability of phenylphosphonic acid, $\text{H}_5\text{C}_6\text{-P}(\text{OH})_2\text{O}$, and phenylthiophosphonic acid, $\text{H}_5\text{C}_6\text{-P}(\text{OH})_2\text{S}$. We carried out DFT and *ab initio* MP2 optimizations [16] of the equilibrium geometries for the stable conformers of the molecules. The data indicate that here the planar form is a saddle point, while a non (near)-planar structure is the only stable conformer in each case (due to the C_{2v} symmetry of the phenyl ring). From our results we can conclude that conjugation effects are almost absent in these compounds, and that their stabilities are mainly determined by electrostatic and steric effects. Additionally, vibrational frequencies were calculated on DFT level, and a complete assignment was made for all the normal modes by employing normal coordinate calculations following [17]. Experience tells us that DFT can predict vibrational spectra very well. We also used the vibrational data to plot the IR (infrared) and Raman spectra of the molecules. The results for phenylphosphonic acid and for phenylthiophosphonic acid are presented in this work and in case of the phosphonic acid are compared to the experimental spectra. For phenylthiophosphonic acid we present a theoretical prediction of the vibrational spectra and the assignment of the spectral lines. The Raman intensities were calculated according to literature methods [18, 19]. Our interest in organophosphorus compounds arose because of the importance of such compounds in chemistry [20–25]. Importantly, such phosphorus compounds have become very interesting also for the chemical industry, *e.g.* as starting materials for drug synthesis, polymer additives, flame retardants, and metal extractants [26].

For our calculations we used the valence triple zeta basis set with polarization functions on all atoms,

i.e. 6-311G**. Our previous calculations [27, 28] have suggested that this basis set is superior to the larger 6-311+G** or 6-311++G** basis sets which include diffuse functions and seem to be not very well balanced, while the smaller 6-311G** basis works quite well in a series of halo- and dihalovinyl methanes, silanes, and germanes.

Results and Discussion

DFT and *ab initio* calculations

The GAUSSIAN98 program [16] running on an IBM RS/6000 43P model 260 workstation was used to carry out the LCAO-MO-SCF calculations at DFT and MP2/6-311G** levels. The structures of the molecules in their most stable conformations together with the atom numbering adopted are shown in Fig. 1.

They were optimized by minimizing the energy with respect to all the geometrical parameters. This optimization (both with DFT and with MP2) directly converged to a planar form. However, a calculation of vibrational frequencies on this structure showed an imaginary one, indicating that the optimization had converged to a maximum along one of the internal coordinates. By relaxing all symmetry constraints and starting the optimization away from the planar geometry, a true minimum was obtained for which all frequencies turned out to be real and positive. A second minimum does not exist. The perpendicular and the planar structures are maxima, the latter one with a very low barrier of only $0.60 \text{ kcal mol}^{-1}$ in the phosphonic acid and $0.65 \text{ kcal mol}^{-1}$ in the thiophosphonic acid. The calculated structural parameters, total energies, rotational constants, rotational barriers and dipole moments of the two molecules are listed in Table S1 (Supporting Information available online only; see note at the end of the manuscript). We could only find

Phenyl derivatives (C_1 symmetry, X = O or S)

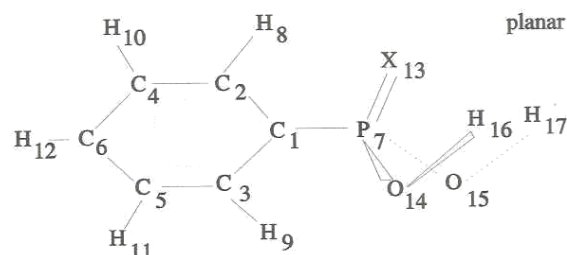


Fig. 1. Atom numbering in the phenyl derivatives under study (for ease of drawing the minimum non (near)-planar structure is not shown).

experimental geometrical data for vinylchlorophosphine oxide and sulfide [29–31], but not for the acids or phenyl derivatives. From the calculations the barrier to rotation through the perpendicular transition state is 2.1 kcal mol⁻¹ in the normal acid, but only 0.87 kcal mol⁻¹ in the thioacid (see Table S2). The extremely small rotational barrier over the planar transition state is probably hard to detect experimentally and is so small because it involves only a slight rotation of the P(OH)₂X (X = O or S) group, and also the O–H bonds are not rotated far out of the *syn* position with respect to the P=X bond. The reason for the non (near)-planar energy minimum must be too close a contact between the strongly negative X atoms and the also negatively polarized carbon atoms in the ring (see Table S3), which an attraction by the positively charged hydrogens in the ring cannot counterbalance. Probably there is also some steric hindrance between the X atom and those hydrogens. Note, that the OPCC dihedral angle is 5.25°, while the SPCC angle is 12.34° due to the size of the sulfur atom.

Torsional potential function

The potential function scan for the internal rotation about the C–P single bond was obtained by allowing the CCPX dihedral angle to vary by 15° increments from 0° (planar position) to 90° (perpendicular position). Full geometry optimizations at each of the fixed CCPO dihedral angles (Φ) of, 15°, 30°, 45°, 75°, and 90° (further calculations were not necessary because of the symmetry of the systems) were carried out at the DFT and MP2/6-311G** levels of calculations. However, it turned out that especially at the lower values of the CCPX angle wild, more or less undamped oscillations in the HOPX angles showed up, making the computation times for these values of the CCPX angle larger than the time limit for calculations. In order to be able to perform the calculations, we had to fix the HOPX angles in the *syn* position relative to the P=X bond (0°) and to optimize only the other internal coordinates for each CCPX angle. This torsional potential function was then represented as a Fourier cosine series in the dihedral angle (Φ):

$$V(\phi) = V_0 + \sum_{n=1}^N \frac{V_n}{2} [1 - \cos(n\phi)] \quad (1)$$

where the potential coefficients from V_0 to V_6 ($N = 6$) are considered adequate to describe the potential

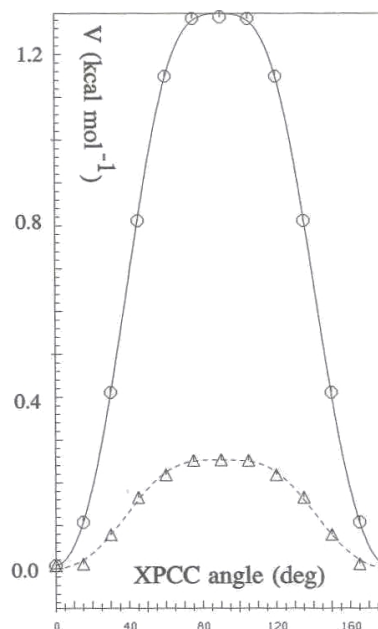


Fig. 2. DFT potential scans (6-311G** basis set) along the $X_{13}P_7C_1C_3$ (X = O or S) dihedral angle for phenylphosphonic acid (solid line, actually calculated DFT points are hexagons) and phenylthiophosphonic acid (dashed line, actually calculated DFT points are triangles). The phosphonic acid curve is relative to -800.105241 Hartrees (root mean square deviation, rms = 4.4 cal mol⁻¹ for the 6th order fit) while the thiophosphonic acid curve is relative to -1123.065214 Hartrees (rms = 5.7 cal/mol for the 6th order fit). The HOPO angles were kept fixed at 0°.

function (as shown by the root mean square deviations, rms, of the least-squares fitting, which were 4.4 and 5.7 cal mol⁻¹, respectively, for the phosphonic and the thiophosphonic acid). The results of the energy optimizations were used to calculate the six coefficients by least-squares fitting. However, the potential curves calculated with fixed HOPX angles suggest a minimum (Fig. 2) in the planar geometry, and therefore we do not list the calculated potential coefficients.

Due to the symmetry of the phenyl ring the potentials are symmetric with respect to the perpendicular (pp) transition state (TS, $\Phi = 90^\circ$) as shown in Fig. 2. In the figure we show the potential functions which are symmetric around a dihedral angle of 90°. The differences between DFT and MP2 calculations are unimportant (compare Table 2), and thus we do not show the MP2 potential functions. The minimum and its equivalent counterpart near the 180° CCPX angle would correspond to a near-*cis* and a near-*trans* conformer in an asymmetric vinyl system, however, due to the sym-

Description	Symmetry coordinate
β -CH	antisymmetric stretch $S_1 = r_3 - r_{11}$
β -CH	symmetric stretch $S_2 = r_3 + r_{11}$
γ -CH	antisymmetric stretch $S_3 = r_5 - r_9$
γ -CH	symmetric stretch $S_4 = r_5 + r_9$
δ -CH	stretch $S_5 = r_7$
	Ring-P stretch $S_6 = A$
β -CH	bend (in-plane) $S_7 = v_1 - v_2 + v_3 - v_4$
β -CH	bend (in-plane) $S_8 = v_1 - v_2 - v_3 + v_4$
γ -CH	bend (in-plane) $S_9 = v_5 - v_6 + v_7 - v_8$
γ -CH	bend (in-plane) $S_{10} = v_5 - v_6 - v_7 + v_8$
δ -CH	bend (in-plane) $S_{11} = v_9 - v_{10}$
	Ring breathing $S_{12} = R_1 + R_2 + R_3 + R_4 + R_5 + R_6$
	Ring deformation $S_{13} = R_1 + R_2 - 2R_3 + R_4 + R_5 - 2R_6$
	Ring deformation $S_{14} = R_1 + R_2 - R_4 - R_5$
	Ring deformation $S_{15} = R_1 - R_2 + R_3 - R_4 + R_5 - R_6$
	Ring deformation $S_{16} = R_1 - R_2 + R_4 - R_5$
	Ring deformation $S_{17} = R_1 - R_2 - 2R_3 - R_4 + R_5 + 2R_6$
	Ring deformation $S_{18} = \alpha_1 - \alpha_2 + \alpha_3 - \alpha_4 + \alpha_5 - \alpha_6$
	Ring deformation $S_{19} = 2\alpha_1 - \alpha_2 - \alpha_3 + 2\alpha_4 - \alpha_5 - \alpha_6$
	Ring deformation $S_{20} = \alpha_2 - \alpha_3 + \alpha_5 - \alpha_6$
O-H	symmetric stretch $S_{21} = T_1 + T_2$
P=X	stretch $S_{22} = B$
PO ₂	symmetric stretch $S_{23} = s_1 + s_2$
POH	symmetric bending $S_{24} = \sigma_1 + \sigma_2$
POH	symmetric wag $S_{25} = \varphi_1 - \varphi_2$
PO ₂	deformation (scissor) $S_{26} = 4\delta - \varepsilon_1 - \varepsilon_2 - \pi_1 - \pi_2$
PO ₂	rock $S_{27} = \varepsilon_1 - \varepsilon_2 + \pi_1 - \pi_2$
	Ring-P bend (in-plane) $S_{28} = \beta_1 - \beta_2$
	Ring-PX bend (in-plane) $S_{29} = 5\theta - \varepsilon_1 - \varepsilon_2 - \pi_1 - \pi_2 - \delta$
β -CH	deformation $S_{30} = \lambda_1$
β -CH	and Ring-P deformation $S_{31} = \lambda_2$
β -CH	and Ring-P deformation $S_{32} = \eta_2$
γ -CH	deformation $S_{33} = \lambda_3$
γ -CH	and δ -CH deformation $S_{34} = \lambda_4 \cos \Phi + \eta_1 \sin \Phi$
γ -CH	and δ -CH deformation $S_{35} = -\lambda_4 \sin \Phi + \eta_1 \cos \Phi$
	Ring deformation $S_{36} = \kappa_1 - \kappa_2 + \kappa_3 - \kappa_4 + \kappa_5 - \kappa_6$
	Ring deformation $S_{37} = \kappa_1 - \kappa_3 + \kappa_4 - \kappa_6$
	Ring deformation $S_{38} = \kappa_1 - 2\kappa_2 + \kappa_3 + \kappa_4 - 2\kappa_5 + \kappa_6$
	antisymmetric torsion $S_{39} = \tau$
O-H	antisymmetric stretch $S_{40} = T_1 - T_2$
PO ₂	antisymmetric stretch $S_{41} = s_1 - s_2$
POH	antisymmetric bending $S_{42} = \sigma_1 - \sigma_2$
POH	antisymmetric wag $S_{43} = \varphi_1 + \varphi_2$
PO ₂	wag $S_{44} = \varepsilon_1 + \varepsilon_2 - \pi_1 - \pi_2$
PO ₂	twist $S_{45} = \varepsilon_1 - \varepsilon_2 - \pi_1 + \pi_2$

Table 1. Symmetry coordinates (not normalized; $\Phi = +15^\circ$) for phenylphosphonic (X = O) and phenylthiophosphonic (X = S) acid.

metry of the phenyl ring they are equivalent. As expected, rotational barriers for the thiophosphonic acid are much lower than those for the phosphonic acid, because an S atom, being less electronegative than an O atom, leads to a much smaller charge separation in the PS bond as compared to the PO bond.

The fact that we have no planar minima indicates that conjugation between the ring and the PX bonds are negligible. Our detailed previous study on vinyl dichlorophosphine oxide and sulfide [32] has shown that conjugation effects due to P=O and C=C bonds

are, if present at all, negligible as it is the case in our acids. Furthermore, Laguna *et al.* [33] have stated that the PO bond is best viewed as a highly polarized triple bond and not capable of conjugation. Their conclusion was based on an investigation of localized orbitals. Thus we do not expect conjugation to play a major role in the structural stability of the acid conformers. Because of the fact that all heavy atoms around the phosphorus atom are negatively charged (hydrogens and phosphorus being positive) we conclude that a large part of the stabilization of the non (near)-planar min-

k	I	A	ρ	PED
33.1	0.5	5.6	0.75	97 % S ₃₉
109.4	1.6	6.0	0.75	63 % S ₃₂ , 12 % S ₃₇ , 12 % S ₄₄ , 11 % S ₄₅
149.2	0.7	0.2	0.73	55 % S ₂₈ , 29 % S ₂₉ , 10 % S ₂₇
192.3	67.6	2.4	0.71	32 % S ₄₃ , 26 % S ₂₅ , 19 % S ₂₆ , 16 % S ₄₅
228.1	59.3	0.6	0.75	30 % S ₂₅ , 23 % S ₄₃ , 16 % S ₄₅ , 14 % S ₂₆
290.9	8.8	5.9	0.35	39 % S ₆ , 21 % S ₂₇ , 21 % S ₁₉
298.0	20.6	2.0	0.74	31 % S ₂₅ , 31 % S ₃₇ , 22 % S ₄₅ , 15 % S ₄₄
361.7	38.8	0.4	0.37	27 % S ₄₃ , 26 % S ₂₉ , 20 % S ₂₈ , 12 % S ₂₆
400.0	42.6	1.9	0.74	34 % S ₄₄ , 29 % S ₄₅ , 13 % S ₃₇ , 11 % S ₂₅
408.2	0.3	0.1	0.70	92 % S ₃₈
450.4	35.7	1.0	0.71	37 % S ₂₆ , 17 % S ₂₇ , 16 % S ₄₃ , 11 % S ₂₉
505.2	148.9	1.9	0.19	34 % S ₂₇ , 18 % S ₁₉ , 17 % S ₂₉
514.5	40.6	0.6	0.74	32 % S ₃₂ , 26 % S ₄₄ , 16 % S ₃₇
632.3	0.1	5.2	0.75	90 % S ₂₀
709.5	35.6	0.2	0.41	61 % S ₃₆ , 18 % S ₃₂ , 10 % S ₃₁
716.4	6.9	11.5	0.06	48 % S ₁₉ , 21 % S ₆
761.4	41.2	0.3	0.75	67 % S ₃₅ , 12 % S ₃₆ , 11 % S ₃₁
833.7	217.4	6.8	0.09	79 % S ₂₃
863.9	12.6	0.9	0.73	50 % S ₃₃ , 45 % S ₃₀
876.4	293.4	1.0	0.59	82 % S ₄₁
943.4	0.8	0.1	0.64	63 % S ₃₁ , 20 % S ₃₅ , 12 % S ₃₄
993.3	0.1	0.0	0.55	45 % S ₃₀ , 36 % S ₃₃ , 13 % S ₃₄
1011.6	65.7	6.2	0.20	50 % S ₂₄ , 20 % S ₁₈ , 19 % S ₄₂
1015.5	0.5	1.9	0.11	70 % S ₃₄ , 12 % S ₃₁
1017.0	22.2	26.8	0.14	35 % S ₁₂ , 30 % S ₂₄ , 25 % S ₁₈
1019.9	65.2	4.6	0.22	62 % S ₄₂ , 12 % S ₁₂
1048.1	1.2	8.2	0.09	42 % S ₁₄ , 22 % S ₁₈ , 15 % S ₁₂ , 11 % S ₉
1101.4	3.5	0.3	0.72	53 % S ₁₇ , 20 % S ₈ , 13 % S ₁₁
1141.2	73.8	9.6	0.11	23 % S ₆ , 20 % S ₁₂ , 18 % S ₁₄ , 16 % S ₁₈
1184.2	0.2	4.0	0.75	39 % S ₁₀ , 36 % S ₁₁ , 13 % S ₁₅
1206.2	1.2	4.1	0.71	38 % S ₉ , 37 % S ₇ , 25 % S ₁₃
1282.6	214.1	11.5	0.11	87 % S ₂₂
1323.6	4.6	0.0	0.14	64 % S ₁₅ , 17 % S ₁₀
1353.1	1.8	0.2	0.74	59 % S ₈ , 19 % S ₁₅
1471.8	20.5	0.5	0.73	32 % S ₁₇ , 29 % S ₁₀ , 29 % S ₁₁
1517.2	1.4	0.1	0.40	34 % S ₉ , 32 % S ₇ , 32 % S ₁₂
1618.8	0.3	5.7	0.75	70 % S ₁₆ , 11 % S ₁₁
1637.2	6.0	26.0	0.64	68 % S ₁₃ , 13 % S ₇
3166.4	0.6	49.6	0.74	52 % S ₅ , 42 % S ₄
3177.4	5.9	120.0	0.75	66 % S ₃ , 30 % S ₁
3184.2	10.1	52.4	0.56	48 % S ₂ , 32 % S ₅ , 13 % S ₄
3192.8	10.9	34.6	0.13	63 % S ₁ , 26 % S ₃
3197.1	10.7	291.2	0.13	42 % S ₂ , 38 % S ₄ , 11 % S ₅
3822.7	111.9	197.1	0.32	53 % S ₄₀ , 47 % S ₂₁
3834.4	120.4	74.8	0.24	53 % S ₂₁ , 47 % S ₄₀

Table 2. Theoretical wavenumbers, k (cm^{-1}), infrared intensities, I (km mol^{-1}), Raman activities A ($\text{\AA}^4 \text{amu}^{-1}$), depolarization ratios ρ , as calculated with the DFT/B3LYP method in a 6-311G** basis set, and the potential energy distribution among the symmetry coordinates, PED (only those larger than 10 % are given), calculated with our program for non-planar phenylphosphonic acid.

imum is of electrostatic nature. However, also steric effects must not be excluded.

Vibrational frequencies and normal coordinate analyses

Our molecules in their non (near)-planar conformations have C_1 symmetry, and the vibrational modes span the irreducible representation 45 A and should be polarized in the Raman spectra of the liquids. Normal coordinate analyses were carried out for the sta-

ble non (near)-planar conformers of the molecules in order to provide a complete assignment of the fundamental vibrational frequencies. A computer program was written by one of us (W.F.) for this purpose following Wilson's method [17]. The cartesian coordinates for the stable conformers together with the normal modes (in cartesian coordinates) and the frequencies from the GAUSSIAN98 output were used as input in the program. An over-complete set of internal coordinates (Table S4) was used to form symmetry coordinates (Table 1). Our program automatically detects re-

<i>k</i>	<i>I</i>	<i>A</i>	ρ	PED
17.5	0.3	4.2	0.75	100 % S ₃₉
107.2	1.9	4.8	0.75	53 % S ₃₂ , 14 % S ₃₇ , 11 % S ₄₄ , 11 % S ₂₉
125.1	2.8	1.2	0.75	43 % S ₂₉ , 23 % S ₂₈
173.5	48.4	1.2	0.33	47 % S ₄₃ , 26 % S ₂₈ , 18 % S ₂₆
217.9	36.1	2.0	0.75	53 % S ₄₅ , 36 % S ₂₅
254.4	22.2	6.2	0.36	25 % S ₆ , 25 % S ₂₇ , 16 % S ₂₉ , 11 % S ₁₉
303.7	10.3	4.0	0.71	34 % S ₃₇ , 29 % S ₄₄ , 20 % S ₂₅
324.2	75.0	5.0	0.66	38 % S ₂₅ , 24 % S ₄₄ , 17 % S ₄₅
331.6	13.5	1.5	0.74	24 % S ₂₈ , 22 % S ₄₃ , 12 % S ₂₆ , 10 % S ₂₉
396.9	41.1	4.8	0.34	33 % S ₂₇ , 19 % S ₂₆ , 17 % S ₂₂ , 14 % S ₄₃
407.9	0.2	0.1	0.74	94 % S ₃₈
453.8	42.9	2.2	0.24	32 % S ₂₆ , 15 % S ₁₉ , 15 % S ₂₉ , 13 % S ₆
506.8	9.7	0.8	0.71	43 % S ₃₂ , 21 % S ₃₇ , 16 % S ₄₄
630.0	20.6	10.4	0.42	75 % S ₂₀ , 11 % S ₂₂
638.7	87.7	20.1	0.04	45 % S ₂₂ , 17 % S ₁₉ , 14 % S ₂₀ , 10 % S ₂₃
707.8	34.7	0.3	0.72	61 % S ₃₆ , 19 % S ₃₂ , 10 % S ₃₁
736.5	81.2	1.9	0.75	36 % S ₁₉ , 25 % S ₆ , 14 % S ₂₂
762.7	43.7	0.3	0.75	67 % S ₃₅ , 12 % S ₃₆ , 11 % S ₃₁
846.2	209.8	1.6	0.27	64 % S ₂₃ , 22 % S ₄₁
861.8	73.3	1.9	0.55	35 % S ₃₃ , 32 % S ₃₀ , 15 % S ₄₁ , 13 % S ₂₃
865.5	172.3	0.7	0.50	55 % S ₄₁ , 16 % S ₃₃ , 13 % S ₃₀
944.0	1.0	0.1	0.54	65 % S ₃₁ , 22 % S ₃₅ , 13 % S ₃₄
992.6	0.1	0.2	0.55	47 % S ₃₀ , 41 % S ₃₃
1014.9	8.3	21.0	0.10	37 % S ₁₈ , 26 % S ₃₄ , 24 % S ₁₂
1015.7	1.9	13.3	0.12	53 % S ₃₄ , 18 % S ₁₈ , 15 % S ₁₂
1018.7	107.2	1.7	0.41	82 % S ₄₂
1033.7	167.8	4.1	0.19	79 % S ₂₄
1047.9	13.4	13.4	0.11	40 % S ₁₄ , 18 % S ₁₈ , 15 % S ₁₂ , 11 % S ₉
1106.7	1.7	0.3	0.71	53 % S ₁₇ , 18 % S ₈ , 14 % S ₁₁
1133.5	73.7	14.4	0.13	25 % S ₆ , 21 % S ₁₄ , 21 % S ₁₂ , 15 % S ₁₈
1184.8	0.2	4.5	0.75	39 % S ₁₀ , 35 % S ₁₁ , 13 % S ₁₅
1210.3	3.7	5.9	0.75	37 % S ₇ , 37 % S ₉ , 26 % S ₁₃
1322.6	3.2	0.4	0.70	69 % S ₁₅ , 16 % S ₁₀
1355.3	5.2	3.0	0.31	62 % S ₈ , 15 % S ₁₅ , 10 % S ₁₁
1471.1	24.6	2.0	0.40	33 % S ₁₇ , 29 % S ₁₀ , 28 % S ₁₁
1516.3	2.4	0.5	0.56	35 % S ₇ , 33 % S ₉ , 32 % S ₁₄
1617.9	1.8	4.4	0.72	68 % S ₁₆ , 11 % S ₁₁
1634.2	3.1	39.2	0.58	66 % S ₁₃ , 12 % S ₇ , 11 % S ₉ , 10 % S ₁₉
3168.0	0.6	52.7	0.75	53 % S ₅ , 41 % S ₄
3179.3	5.9	121.3	0.74	70 % S ₃ , 29 % S ₁
3185.6	6.6	55.1	0.47	53 % S ₂ , 32 % S ₅ , 14 % S ₄
3193.9	9.6	6.6	0.74	70 % S ₁ , 29 % S ₃
3197.8	13.4	320.4	0.13	45 % S ₄ , 41 % S ₂ , 14 % S ₅
3809.2	107.5	150.4	0.29	53 % S ₄₀ , 47 % S ₂₁
3830.2	119.2	59.9	0.23	53 % S ₂₁ , 47 % S ₄₀

Table 3. Theoretical wavenumbers, *k* (cm⁻¹), infrared intensities, *I* (km mol⁻¹), Raman activities *A* (Å⁴ amu⁻¹), depolarization ratios ρ , as calculated with the DFT/B3LYP method in a 6-311G** basis set, and the potential energy distribution among the symmetry coordinates, PED (only those larger than 10 % are given), calculated with our program for non-planar phenylthiophosphonic acid.

dundant internal coordinates and eliminates them from the symmetry coordinates.

The normal modes were next transformed to mass-weighted cartesian coordinates, which were then used to calculate the force constant matrix. This was diagonalized, and its eigenvectors and eigenvalues were used in the further calculations. Following this step the force constant matrix was transformed to internal coordinates. To ensure correctness, this transformation is checked in the program numerically in both directions.

At this point the force constant matrix in internal coordinates could be scaled if desired, back-transformed to mass-weighted cartesians and diagonalized again to get scaled frequencies and normal modes. The matrix was finally transformed to symmetry coordinates where again all possible numerical checks were performed.

In the next step the normal modes were also transformed to symmetry coordinates. Finally, the potential energy distribution (PED) for each normal mode among the symmetry coordinates of the molecules

in their stable conformation was calculated. A complete assignment of the fundamentals was proposed. The assignments were made based on calculated PED, infrared band intensities, Raman line activities and depolarization ratios, and experimental data for phenylphosphonic acid. The data of the vibrational assignments for phenylphosphonic acid are given in Table 2, those for phenylthiophosphonic acid in Table 3.

As is obvious from the Table, the normal modes in our phenyl-substituted rings are mostly not very pure symmetry coordinates, but mix several of them together. The antisymmetric torsion is a pure vibration in both acids with very small wave numbers (33 and 17 cm^{-1}). These small wavenumbers are a further indication for the absence of conjugation, which would imply larger ones, if present. Further they explain the difficulties in the optimizations. The following modes are highly mixed, with three to four symmetry coordinates involved. Relatively intense bands among them in the IR spectrum are calculated around 200 cm^{-1} and contain mainly POH symmetric and antisymmetric wags, both in the phosphonic and in the thiophosphonic molecule. The most intense Raman line is for both molecules the antisymmetric torsion, which is so high that the others can be seen mostly just in an enlarged inset (see below). Another rather intense feature is calculated around 400 cm^{-1} again for both molecules, containing PO₂ twist and wag.

Besides the antisymmetric torsion the second highest line in the Raman spectra is the pure ring breathing around 1000 cm^{-1} , which in the thio derivative is mixed with other ring deformations. In the phosphonic acid rather pure normal modes can be found at 408 (92 % S₃₈, another ring deformation), 834 (79 % S₂₃ PO₂ symmetric stretch), 876 (82 % S₄₁, PO₂ antisymmetric stretch), and 1283 cm^{-1} (87 % S₂₂ P = O stretch), most of them with rather large transmittance. In the thiophosphonic acid rather pure normal modes can be found at 408 (94 % S₃₈, another ring deformation), 1019 (82 % S₄₂ POH antisymmetric bend), and 1034 cm^{-1} (79 % S₂₄, POH symmetric bend), most of them with rather large transmittance. In the thiophosphonic acid the degree of mixing is somewhat higher than in the phosphonic acid.

Calculation of replotted experimental vibrational spectra

The methods used for the calculation of theoretical vibrational spectra from the data provided by GAUS-

SIAN98 are outlined briefly in the Appendix contained in the Supporting Information (available online only; see note at the end of the manuscript). Here we want to show shortly the way of replotting experimental spectra found in the literature. In order to obtain comparable spectra from our experimental one [34] and the theoretical infrared and Raman spectra of the phosphonic acid, we have replotted the experimental spectrum. We obtained the wavenumbers and peak intensities for each line from the experimental infrared spectrum, and in order to replot it we have assumed a constant line width $\Delta k = 10 \text{ cm}^{-1}$ in both spectra. For the experimental one we assumed a Lorentzian line shape for each of the lines, j ,

$$L_j(k) = \frac{A_j}{\pi} \frac{\Delta k/2}{(k - k_j)^2 + (\Delta k/2)^2} \quad (2)$$

where the peak heights I_j can be measured from the experimental spectra and thus

$$I_j = L_j(k_j) = \frac{A_j}{\pi \Delta k/2} \quad (3)$$

and from this follows

$$A_j = \frac{1}{2} I_j \Delta k \pi \quad (4)$$

where I_j is the distance between the peak of the line and the base line of the experimental spectrum. The final spectrum is then the superposition of all experimental lines j

$$T(k) = - \sum_j \frac{I_j \Delta k/2}{(k - k_j)^2 + (\Delta k/2)^2} \quad (5)$$

and $T(k)$ is rescaled such that the largest absolute value of the transmittance is equal to unity. The Raman spectrum is treated in the same way, just with intensity instead of transmittance.

Discussion of spectra

In Fig. 3 we show the calculated infrared (IR) spectrum together with the experimental one, replotted from the website [34] as described above for the stable non (near)-planar conformer of phenylphosphonic acid.

As mentioned above, the largest IR intensities belong clearly to the bands in the skeletal or fingerprint region of the molecule. Note, that the spectrum

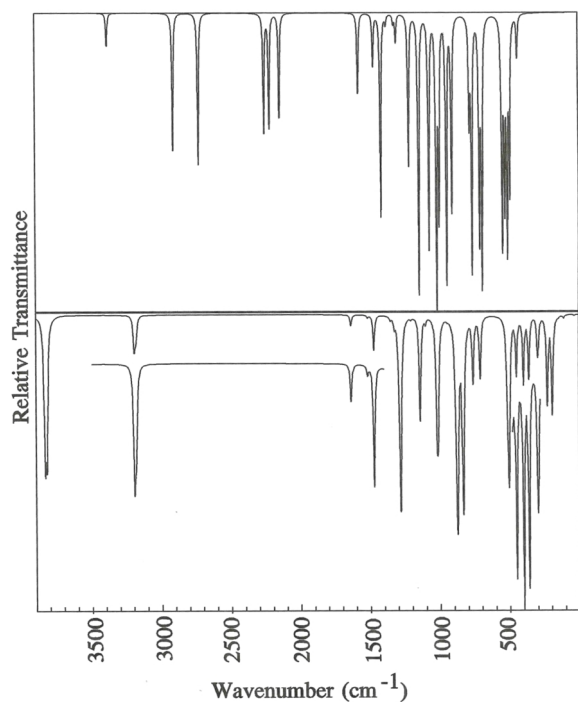


Fig. 3. Infrared spectrum of phenylphosphonic acid as calculated with the DFT/B3LYP method in a 6-311G** basis set (lower panel) and the experimental spectrum (upper panel) which starts out at around 400 cm^{-1} and is replotted with a line width of 10 cm^{-1} in order to be better comparable with our theoretical spectrum.

was recorded only above about 400 cm^{-1} . In the region of $200\text{--}500\text{ cm}^{-1}$, wavenumbers are calculated which belong to a considerable extent to motions of the PO_2 group, namely wag, twist, scissor, and rock. We expect them to have some intensity because of the charge separation in the P–O bonds of about $+e$ at P and -0.5 e at O. We have to assign the rather intense and closely spaced group of bands around 500 cm^{-1} in the experimental spectrum to those motions. The corresponding group of lines in the calculated spectrum is not that closely spaced and tends to be a bit lower in frequency. One of the most intense bands both theoretically and experimentally is the P=O stretch in the phosphonic and the P=S stretch in the thiophosphonic acid, which is a pure normal mode in the former at about 1300 cm^{-1} and a mixed one in the latter at about 850 cm^{-1} . This is again due to the polarization of the P=X group which is about $+e$ for P and about -0.58 e for O in the phosphonic and about -0.45 e for S in the thiophosphonic acid, the charge on S being less than that on O, due to the larger elec-

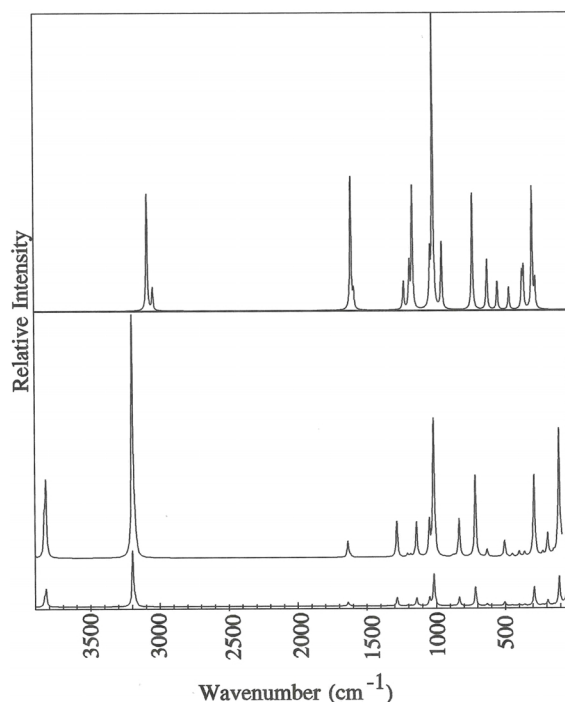


Fig. 4. Raman spectrum of phenylphosphonic acid as calculated with the DFT/B3LYP method in a 6-311G** basis set (lower panel) and the experimental spectrum (upper panel) which starts out at around 250 cm^{-1} and is replotted with a line width of 10 cm^{-1} in order to be better comparable with our theoretical spectrum.

tronegativity of O. The mode is lower in wavenumber for P=S than for P=O because the PS bond is weaker than the PO bond. Ring deformations are calculated between 1300 and 1650 cm^{-1} and are quite intense features also in the experimental spectrum. The most intense and characteristic line of those is as expected the one at 1017 cm^{-1} for phenylphosphonic acid which is 35% ring breathing, S_{12} .

The two bands which are highest in wavenumber are composed from O–H symmetric and antisymmetric stretch. The bands are a broad feature in the experimental spectrum, which cannot be seen in our replot because there we assign a line width of 10 cm^{-1} to all the bands. However, it has to be noted that the intensity of the O–H stretches in the experimental IR spectrum is lower than expected for a normal organic acid. This indicates that hydrogen bonding is rather weak in the system, so that mainly the bands of the dimer contribute to that feature. The reason for that must be the steric requirements of the phenyl ring.

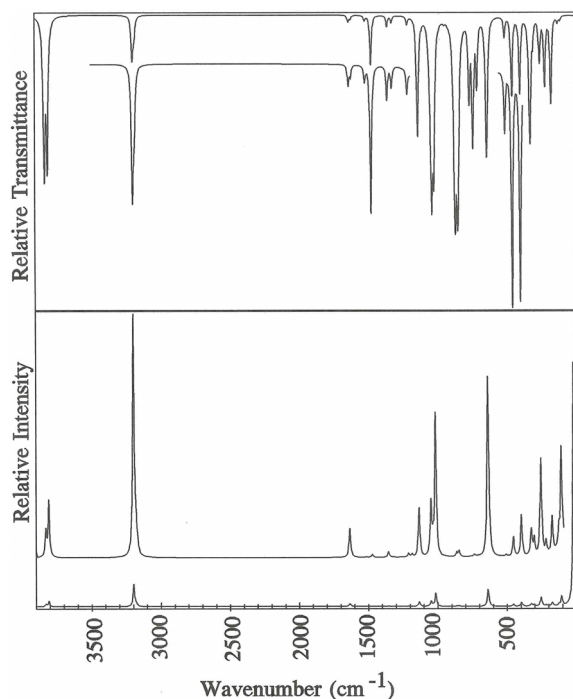


Fig. 5. Infrared (upper panel) and Raman (lower panel) spectra of the stable non (near)-planar conformer of phenylthiophosphonic acid as calculated with the DFT/B3LYP method in a 6-311G** basis set.

The theoretical and experimental [34] Raman spectra for the phosphonic acid are shown in Fig. 4.

In the calculated Raman spectra of the two compounds the largest intensity is calculated at the line corresponding to the antisymmetric torsion, being so high in intensity that the other lines can be seen only in an enlarged inset. This effect is not seen in the experimental Raman spectrum of the phosphonic acid, because there recording starts only above roughly 200 cm^{-1} .

As expected, the second highest intensity (highest in experiment) occurs at ring motions (which lead to the largest changes in polarizability) around 1000 cm^{-1} , both theoretically and experimentally at roughly the same wavenumber.

Since theory reproduces the experimental spectra rather well for phosphonic acid, we show in Fig. 5 the theoretical spectra for the thiophosphonic acid.

The general appearance of the spectra is very reasonable as discussed above, and we are in no doubt that Fig. 5 is a reasonable prediction of those spectra. Also the assignments given in Table 3 we expect to be rather correct.

Conclusion

One of our main conclusion is that the structural properties of the phenylphosphonic and phenylthiophosphonic acids are dominated not by conjugation but by electrostatic and steric effects. Vibrational spectra are reproduced rather well by DFT calculations for the phosphonic acid, which leads us to the conclusion that our prediction of the vibrational spectra of the thiophosphonic acid should be a reasonable one, as well as the assignments.

Supporting information

Tables S1–S4 and an Appendix “Calculation of Theoretical Vibrational Spectra” are provided as Supporting Information online only (<http://www.znaturforsch.com/ab/v65b/c65b.htm>).

Acknowledgement

Support by King Fahd University of Petroleum and Minerals (KFUPM) and the Chemistry Department at KFUPM is greatly acknowledged.

- [1] J. Keirns, R.F. Curl, Jr., *J. Chem. Phys.* **1978**, *48*, 3773.
- [2] R.G. Latypova, A.K. Mamleev, L.N. Gunderova, N.M. Pozdeev, *Zh. Strukt. Khim.* **1976**, *17*, 849.
- [3] J.R. Durig, J.S. Church, D.A.C. Compton, *J. Chem. Phys.* **1979**, *71*, 1175.
- [4] J.R. Durig, P.A. Brletic, J.S. Church, *J. Chem. Phys.* **1982**, *76*, 1723.
- [5] B.C. Laskowski, R.L. Jaffe, A. Komornicki, *J. Chem. Phys.* **1985**, *82*, 5089.
- [6] J.R. Durig, R.J. Berry, P. Groner, *J. Chem. Phys.* **1987**, *87*, 6303.
- [7] J.R. Durig, A.Y. Wang, T.S. Little, *J. Chem. Phys.* **1989**, *91*, 7361.
- [8] J.R. Durig, A.Y. Wang, T.S. Little, *J. Chem. Phys.* **1990**, *93*, 905.
- [9] J.R. Durig, P.A. Brletic, Y.S. Li, A.Y. Wang, T.S. Little, *J. Mol. Struct.* **1990**, *223*, 291.
- [10] J.R. Durig, C.V. Groner, T.G. Costner, A.Y. Wang, *J. Raman Spectrosc.* **1993**, *24*, 335.
- [11] G.R. De Mare, Y.N. Panchenko, *J. Phys. Chem.* **1994**, *98*, 8315.
- [12] J.R. Durig, G.A. Guirgis, Y. Jin, *J. Mol. Struct.* **1996**, *380*, 31.

- [13] H. M. Badawi, *J. Mol. Struct. (Theochem)* **1998**, 425, 227.
- [14] H. M. Badawi, W. Förner, *J. Mol. Struct. (Theochem)* **2001**, 535, 103.
- [15] J. Backvall, R. Chinchilla, C. Najera, M. Yus, *Chem. Rev.* **1998**, 98, 2291.
- [16] M. J. Frisch, G. W. Trucks, H. B. Schlegel, G. E. Scuseria, M. A. Robb, J. R. Cheeseman, V. G. Zakrzewski, J. A. Montgomery, Jr., R. E. Stratmann, J. C. Burant, S. Dapprich, J. M. Millam, A. D. Daniels, K. N. Kudin, M. C. Strain, O. Frakas, J. Tomasi, V. Barone, M. Cossi, R. Cammi, B. Mennucci, C. Pomelli, C. Adamo, S. Clifford, J. Ochterski, G. A. Petersson, P. Y. Ayala, Q. Cui, K. Morokuma, D. K. Malick, A. D. Rabuck, K. Raghavachari, J. B. Foresman, J. Cioslowski, J. V. Ortiz, A. G. Baboul, B. B. Stefanov, G. Liu, A. Liashenko, P. Piskorz, I. Komaromi, R. Gomperts, R. L. Martin, T. L. Fox, T. Keith, M. A. Al-Laham, C. Y. Peng, A. Nanayakkara, C. Gonzalez, M. Challacombe, P. M. W. Gill, P. G. Johnson, W. Chen, W. Wong, J. L. Andres, M. Head-Gordon, E. S. Replogle, J. A. Pople, GAUSSIAN98, Gaussian Inc., Pittsburgh, PA (USA) **1998**.
- [17] E. B. Wilson, J. C. Decius, P. C. Cross, *Molecular Vibrations*, McGraw-Hill, New York, **1955**.
- [18] J. R. Durig, G. A. Guirgis, K. A. Krutules, H. Phan, H. D. Stidham, *J. Raman Spectrosc.* **1994**, 25, 221.
- [19] G. W. Chantry, in *The Raman Effect*, Vol. 1 (Ed.: A. Anderson), Marcel Dekker, New York, **1971**, chapter 2.
- [20] J. R. Durig, T. J. Hizer, R. J. Harlan, *J. Chem. Phys.* **1992**, 96, 541.
- [21] K. K. Chatterjee, J. R. Durig, *J. Mol. Struct.* **1995**, 351, 25.
- [22] J. R. Durig, F. D. Daeyaert, *J. Raman Spectrosc.* **1998**, 29, 191.
- [23] E. D. Berning, V. K. Katti, L. C. Barnes, *J. Am. Chem. Soc.* **1999**, 121, 1658.
- [24] J. R. Durig, R. J. Berry, P. Groner, *J. Chem. Phys.* **1987**, 87, 6303.
- [25] J. R. Durig, F. D. Daeyaert, B. J. van der Veken, *J. Raman Spectrosc.* **1994**, 25, 869.
- [26] O. Salama, G. J. Raul, M. Jose, G. de la Vega, *Int. J. Quantum Chem.* **2003**, 91, 333.
- [27] W. Förner, H. M. Badawi, *Coll. Czech. Chem. Comm.* **2007**, 72, 15.
- [28] W. Förner, H. M. Badawi, *Can. J. Anal. Sc. and Spectr.* **2007**, 52, 101.
- [29] V. A. Naumov, S. A. Shagidullin, *Zhur. Strukt. Khim.* **1976**, 17, 304.
- [30] A. V. Chernova, G. M. Doroshkina, S. A. Katsyuba, R. R. Shagidullin, N. A. Khailova, V. K. Khairullin, *Izv. Akad. Nauk SSSR, Ser. Khim.* **1987**, 12, 2729.
- [31] A. V. Chernova, G. M. Doroshkina, S. A. Katsyuba, R. R. Shagidullin, N. A. Khailova, V. K. Khairullin, *Izv. Akad. Nauk SSSR, Ser. Khim.* **1988**, 3, 568.
- [32] W. Förner, H. M. Badawi, *Coll. Czech. Chem. Comm.* **2008**, 73, 831.
- [33] A. Hernandez-Laguna, C. I. Sainz-Diaz, Y. G. Smeyers, J. L. G. de Paz, E. Glavez-Ruano, *J. Phys. Chem.* **1994**, 98, 1109.
- [34] SDBSWeb: <http://riodb01.ibase.aist.go.jp/sdbs/> (National Institute of Advanced Industrial Science and Technology, hit-no.: 5270); SDBS-No. 10133.

Vibrational Spectra of Phenylphosphonic and Phenylthiophosphonic Acid and their Complete Assignment

Wolfgang Förner and Hassan M. Badawi

Department of Chemistry, King Fahd University of Petroleum & Minerals (KFUPM), Dhahran 31261, Saudi Arabia

Supporting Information

Table S1. Calculated structural data, rotational constants, barriers for the rotation between the two non-planar minima through the planar maximum, and dipole moments for non-planar phenylphosphonic acid (PO) and phenylthiophosphonic acid (PS), obtained with the DFT/B3LYP methods and a 6-311G** basis set.

Table S2. Total, E_t , (Hartrees) and relative, E_r , (kcal mol^{-1}) energies as calculated using the MP2 (where available) and DFT method (6-311G** basis set) for the minima (non-planar, np) and transition states (planar, p, and perpendicular at 90° XPCC torsional angle, pp) for phenylphosphonic (PO) and phenylthiophosphonic (PS) acids.

Table S3. The partial charges, Q (in electronic charges), on different atoms obtained by Mulliken population analyses in calculations done by the DFT/B3LYP method using a 6-311G** basis set for the most stable conformers (np) of phenylphosphonic (PO) and phenylthiophosphonic (PS) acids.

Table S4. Internal coordinate definitions (for atom denotation, see Fig. 1) for phenylphosphonic ($X = \text{O}$) and phenylthiophosphonic ($X = \text{S}$) acid.

Table S1. Calculated structural data, rotational constants, barriers for the rotation between the two non-planar minima through the planar maximum, and dipole moments for non-planar phenylphosphonic acid (PO) and phenylthiophosphonic acid (PS), obtained with the DFT/B3LYP methods and a 6-311G** basis set.

	PO (X = O)	PS (X = S)
Bond lengths (Å)		
P ₇ = X ₁₃	1.480	1.945
C ₁ -P ₇	1.800	1.808
P ₇ -O ₁₄	1.631	1.634
P ₇ -O ₁₅	1.614	1.622
C ₁ -C ₂	1.398	1.397
C ₂ -C ₄	1.392	1.391
C ₄ -C ₆	1.395	1.395
C ₆ -C ₅	1.395	1.395
C ₅ -C ₃	1.392	1.391
C ₃ -C ₁	1.398	1.397
H ₈ -C ₂	1.084	1.083
H ₁₀ -C ₄	1.084	1.084
H ₁₂ -C ₆	1.084	1.084
H ₁₁ -C ₅	1.084	1.084
H ₉ -C ₃	1.084	1.083
H ₁₆ -O ₁₄	0.965	0.965
H ₁₇ -O ₁₅	0.965	0.966
Bond angles (deg)		
P ₇ C ₁ C ₂	118.16	120.12
H ₈ C ₂ C ₁	119.16	119.63
H ₉ C ₃ C ₁	120.01	120.06
H ₁₀ C ₄ C ₂	119.95	119.88
H ₁₁ C ₅ C ₃	119.94	119.86
H ₁₂ C ₆ C ₄	119.85	119.89
X ₁₃ P ₇ C ₁	115.26	117.74

(continued on the next page)

Table S1. (continued from previous page)

	PO (X = O)	PS (X = S)
Bond angles (deg)		
O ₁₄ P ₇ C ₁	106.87	104.76
O ₁₅ P ₇ C ₁	101.72	100.75
X ₁₃ P ₇ O ₁₄	113.26	113.63
X ₁₃ P ₇ O ₁₅	117.63	116.77
O ₁₄ P ₇ O ₁₅	100.33	100.95
H ₁₆ O ₁₄ P ₇	110.89	110.99
H ₁₇ O ₁₅ P ₇	112.76	112.14
Dihedral angles (deg)		
X ₁₃ P ₇ C ₁ C ₂	5.25	12.34
O ₁₄ P ₇ C ₁ X ₁₃	126.83	127.36
O ₁₅ P ₇ C ₁ X ₁₃	-128.43	-128.16
H ₁₆ O ₁₄ P ₇ X ₁₃	27.63	18.97
H ₁₇ O ₁₅ P ₇ X ₁₃	52.39	41.76
Rotational constants (GHz)		
A	2.4957	1.9441
B	0.7920	0.6809
C	0.6931	0.5707
Rotational barriers (kcal mol ⁻¹) through the planar state		
	0.60	0.13
Rotational barriers (kcal mol ⁻¹) through the perpendicular state		
	2.10	0.87
Dipole moments (Debye)		
	2.35	2.66

Table S2. Total, E_t , (Hartrees) and relative, E_r , (kcal mol⁻¹) energies as calculated using the MP2 (where available) and DFT method (6-311G** basis set) for the minima (non-planar, np) and transition states (planar, p, and perpendicular at 90 ° XPCC torsional angle, pp) for phenylphosphonic (PO) and phenylthiophosphonic (PS) acids.

System	state	MP2		DFT	
		$E_r(\text{H})$	E_r (kcal mol ⁻¹)	$E_r(\text{H})$	E_r (kcal mol ⁻¹)
PO	np ^a	-798.3524348	0.00	-800.1065514	0.00
	p ^b	-798.3513973	0.65	-800.1055894	0.60
	pp ^c	not located		-800.1032001	2.10
PS	np ^a	-1120.9209828	0.00	-1123.0661919	0.00
	p ^b	-1120.9207203	0.16	-1123.0659806	0.13
	pp ^c	not located		-1123.0648100	0.87

^a Since the two equivalent minima are not perpendicular but near planar, there must be another maximum between the two np minima, but we did not locate it for MP2,

^b in the corresponding frequency calculation always one imaginary frequency appeared, pointing to a maximum,

^c taken from the scans, i.e. the XPOH torsional angles were kept fixed at 0 °.

Table S3. The partial charges, Q (in electronic charges), on different atoms obtained by Mulliken population analyses in calculations done by the DFT/B3LYP method using a 6-311G** basis set for the most stable conformers (np) of phenylphosphonic (PO) and phenylthiophosphonic (PS) acids.

Atom	Q	
	PO (X=O)	PS (X=S)
C ₁	-0.37	-0.36
C ₂	-0.06	-0.05
C ₃	-0.03	-0.01
C ₄	-0.08	-0.09
C ₅	-0.08	-0.09
C ₆	-0.08	-0.08
P ₇	+1.18	+0.92
X ₁₃	-0.58	-0.45
O ₁₄	-0.53	-0.50
O ₁₅	-0.52	-0.49
H ₁₆	+0.30	+0.31
H ₁₇	+0.31	+0.32
H ₈	+0.13	+0.14
H ₉	+0.11	+0.12
H ₁₀	+0.10	+0.10
H ₁₁	+0.10	+0.10
H ₁₂	+0.10	+0.10

Table S4. Internal coordinate definitions (for atom denotation, see Fig. 1) for phenylphos-phonic (X = O) and phenylthiophosphonic (X = S) acid.

No.	Coordinate	Definition	No.	Coordinate	Definition
1	C ₁ -C ₃ stretch	R ₁	33	H ₁₀ C ₄ C ₆ H ₁₂ + H ₁₁ C ₅ C ₆ H ₁₂	torsion λ ₃
2	C ₁ -C ₂ stretch	R ₂	34	H ₁₀ C ₄ C ₆ H ₁₂ - H ₁₁ C ₅ C ₆ H ₁₂	torsion λ ₄
3	C ₂ -C ₄ stretch	R ₃	35	H ₁₂ C ₆ C ₄ C ₅	wag η ₁
4	C ₄ -C ₆ stretch	R ₄	36	P ₇ C ₁ C ₂ C ₃	wag η ₂
5	C ₅ -C ₆ stretch	R ₅	37	C ₃ C ₁ C ₂ C ₄	torsion κ ₁
6	C ₃ -C ₅ stretch	R ₆	38	C ₁ C ₂ C ₄ C ₆	torsion κ ₂
7	C ₁ -P ₇ stretch	A	39	C ₂ C ₄ C ₆ C ₅	torsion κ ₃
8	C ₂ -H ₈ stretch	r ₃	40	C ₄ C ₆ C ₅ C ₃	torsion κ ₄
9	C ₄ -H ₁₀ stretch	r ₅	41	C ₆ C ₅ C ₃ C ₁	torsion κ ₅
10	C ₆ -H ₁₂ stretch	r ₇	42	C ₅ C ₃ C ₁ C ₂	torsion κ ₆
11	C ₅ -H ₁₁ stretch	r ₉	43	P ₇ -X ₁₃	stretch B
12	C ₃ -H ₉ stretch	r ₁₁	44	P ₇ -O ₁₄	stretch s ₁
13	C ₂ C ₁ C ₃ bend	α ₁	45	P ₇ -O ₁₅	stretch s ₂
14	C ₄ C ₂ C ₁ bend	α ₂	46	C ₁ P ₇ X ₁₃	bend θ
15	C ₆ C ₄ C ₂ bend	α ₃	47	O ₁₄ P ₇ X ₁₃	bend π ₁
16	C ₅ C ₆ C ₄ bend	α ₄	48	O ₁₄ P ₇ C ₁	bend π ₂
17	C ₆ C ₅ C ₃ bend	α ₅	49	O ₁₅ P ₇ X ₁₃	bend ε ₁
18	C ₅ C ₃ C ₁ bend	α ₆	50	O ₁₅ P ₇ C ₁	bend ε ₂
19	C ₁ C ₂ H ₈ bend	v ₁	51	O ₁₄ P ₇ O ₁₅	bend δ
20	C ₄ C ₂ H ₈ bend	v ₂	52	(X ₁₃ P ₇ C ₁ C ₂ + antisymmetric torsion τ	
21	C ₁ C ₃ H ₉ bend	v ₃		O ₁₄ P ₇ C ₁ C ₂ +	
22	C ₅ C ₃ H ₉ bend	v ₄		O ₁₅ P ₇ C ₁ C ₂)	
23	C ₂ C ₄ H ₁₀ bend	v ₅	53	O ₁₄ -H ₁₆	stretch T ₁
24	C ₆ C ₄ H ₁₀ bend	v ₆	54	O ₁₅ -H ₁₇	stretch T ₂
25	C ₃ C ₅ H ₁₁ bend	v ₇	55	P ₇ O ₁₄ H ₁₆	bend σ ₁
26	C ₆ C ₅ H ₁₁ bend	v ₈	56	P ₇ O ₁₅ H ₁₇	bend σ ₂
27	C ₄ C ₆ H ₁₂ bend	v ₉	57	O ₁₃ P ₇ O ₁₄ H ₁₆	wag φ ₁
28	C ₅ C ₆ H ₁₂ bend	v ₁₀	58	O ₁₃ P ₇ O ₁₅ H ₁₇	wag φ ₂
29	P ₇ C ₁ C ₂ bend	β ₁			
30	P ₇ C ₁ C ₃ bend	β ₂			
31	H ₈ C ₂ C ₁ P ₇ + H ₉ C ₃ C ₁ P ₇	torsion λ ₁			
32	H ₈ C ₂ C ₁ P ₇ - H ₉ C ₃ C ₁ P ₇	torsion λ ₂			

Appendix: Calculation of Theoretical Vibrational Spectra

For calculation of the Raman spectra we used the scattering activities S_j , the wavenumbers k_j and the depolarization ratios ρ_j for each normal mode j as calculated by the program GAUSSIAN98 [16]. Then the Raman cross sections which are proportional to the intensities are given as [20, 21]

$$\frac{\partial \sigma_j}{\partial \Omega} = \frac{2^4 \pi^4}{45} \frac{h(k_o - k_j)^4}{8\pi^2 c k_j [1 - e^{-\frac{hck_j}{k_B T}}]} S_j \frac{1 - \rho_j}{1 + \rho_j} \quad (\text{A1})$$

Since we are interested only in relative intensities, we calculated them as

$$I_j = \frac{\frac{\partial \sigma_j}{\partial \Omega}}{\frac{\partial \sigma_{j_m}}{\partial \Omega}} \quad (\text{A2})$$

where j_m denotes that line among all the lines from all conformers present in a mixture which has the largest Raman cross section. As laser wavelength we used that of an argon ion laser at $\lambda_o = 514.5$ nm ($k_o = 1/\lambda_o$). As temperature we used $T = 298.15$ K. Then the line shapes are calculated as Lorentzians (L) with a width of $\Delta k = 10$ cm⁻¹ corresponding to the line widths in our replotted experimental spectra used for comparison. Thus the final spectrum for one conformer of a molecule is calculated as

$$I'(k) = \sum_j I_j L(k - k_j); \quad I(k) = \frac{I'(k)}{I_m} \quad (\text{A3})$$

where $I_m = \max[I'(k)]$, and

$$L(k - k_j) = \frac{1}{\pi} \frac{\frac{\Delta k}{2}}{(k - k_j)^2 + \left(\frac{\Delta k}{2}\right)^2}; \quad \int_{-\infty}^{\infty} L(k - k_j) dk = 1 \quad (\text{A4})$$

where the index j runs over all normal modes. For the plots a step size for the grid of generally 10 cm⁻¹ was used. However, when a line appears between two consecutive grid points, N_p extra points with a step size of $\Delta k/(N_p/2)$ are inserted (here $N_p = 12$ is used; note that N_p in the input should be even) into this interval which include the exact center of the line.

The intensities given by the program for infrared (IR) spectra are calculated at all levels of computation used. They represent actually integrated absorption coefficients A_j for the different normal modes j of a system. The Lambert-Beer law tells that at any wavenumber k of an absorption band corresponding to a normal mode j

$$\log_{10} \frac{I}{I_o} = -\varepsilon_j(k)cl \quad (\text{A5})$$

holds, where I is the light intensity after passing through the sample, I_o the incident intensity, $\varepsilon_j(k)$ the molar absorption coefficient for mode j at wavenumber k , c the concentration and l the optical

path length. If c is given in mol cm^{-3} and l in cm , then ε must be expressed in $\text{cm}^2 \text{mol}^{-1}$. Calculation of the integrated absorption coefficient A_j of a line j ,

$$A_j = \int_{-\infty}^{\text{infinity}} \varepsilon_j(k) dk \quad (\text{A6})$$

adds a factor of cm^{-1} to the unit of $\varepsilon_j(k)$ and thus A_j has the unit cm mol^{-1} . However, for a transmittance $T = \log_{10} I/I_0$ of 0.1 in a line of width 0, a concentration of 0.1 mol dm^{-3} and a path length of 1 cm , an integrated absorption coefficient A_j of the order $10,000 \text{ cm mol}^{-1}$ would be needed, and even larger than that if $T = 0.1$ is for the peak transmittance of a line with finite width. Thus the program gives A_j in units of km mol^{-1} , and therefore in this case $A_j = 0.1 \text{ km mol}^{-1}$. Thus in the case of IR lines a Lorentzian shape is given to $\varepsilon_j(k)$:

$$\varepsilon_j(k) = \frac{A_j}{\pi} \frac{\Delta k/2}{(k - k_j)^2 + (\Delta k/2)^2} \quad (\text{A7})$$

where k_j is the band center and Δk the line width as above. Note, that the Lorentzian gives the $\varepsilon_j(k)$ values the correct unit. Then the spectral absorption coefficient for a molecule is calculated as

$$\varepsilon(k) = \sum_j \varepsilon_j(k) = \sum_j \frac{A_j}{\pi} \frac{\Delta k/2}{(k - k_j)^2 + (\Delta k/2)^2} \quad (\text{A8})$$

If there is only one conformer present, the relative transmittance at each wavenumber is calculated as

$$T(k) = 10^{-\varepsilon(k)/\varepsilon_m} \quad (\text{A9})$$

$$\varepsilon_m = \max\{\varepsilon(k)\}$$

Thus ε_m represents $1/(cl)$.